The American Journal of Pathology, Vol. 170, No. 1, January 2007

DOI: 10.2353/ajpath.2007.060687

Musculoskeletal Pathology

Caveolin-1$^{(-/-)}$- and Caveolin-2$^{(-/-)}$-Deficient Mice Both Display Numerous Skeletal Muscle Abnormalities, with Tubular Aggregate Formation

William Schubert,* Federica Sotgia,*†‡
Alex W. Cohen,* Franco Capozza,*‡
Gloria Bonuccelli,*†‡ Claudio Bruno,†
Carlo Minetti,† Eduardo Bonilla,§
Salvatore DiMauro,§ and Michael P. Lisanti *†‡

From the Departments of Molecular Pharmacology and Medicine, Albert Einstein College of Medicine, Bronx, New York; Muscular and Neurodegenerative Disease Unit,† University of Genova and G. Gaslini Pediatric Institute, Genova, Italy; Department of Cancer Biology,‡ Kimmel Cancer Center, Thomas Jefferson University, Philadelphia, Pennsylvania; and H. Houston Merritt Clinical Research Center for Muscular Dystrophy and Department of Neurology,§ Columbia University, College of Physicians and Surgeons, New York, New York*

Here, we examine the role of "non-muscle" caveolins (Cav-1 and Cav-2) in skeletal muscle biology. Our results indicate that skeletal muscle fibers from male Cav-1$^{(-/-)}$ and Cav-2$^{(-/-)}$ mice show striking abnormalities, such as tubular aggregates, mitochondrial proliferation/aggregation, and increased numbers of M-cadherin-positive satellite cells. Notably, these skeletal muscle defects were more pronounced with increasing age. Because Cav-2-deficient mice displayed normal expression levels of Cav-1, whereas Cav-1-null mice exhibited an almost complete deficiency in Cav-2, these skeletal muscle abnormalities seem to be due to loss of Cav-2. Thus, Cav-2$^{(-/-)}$ mice represent a novel animal model—and the first genetically well-defined mouse model—that can be used to study the pathogenesis of tubular aggregate formation, which remains a poorly understood age-related skeletal muscle abnormality. Finally, because Cav-1 and Cav-2 were not expressed within mature skeletal myofibers, our results indicate that development of these abnormalities probably originates in stem/precursor cells, such as satellite cells or myoblasts. Consistent with this hypothesis, skeletal muscle isolated from male Cav-3$^{(-/-)}$ mice did not show any of these abnormalities. As such, this is the first study linking stem cells with the genesis of these intriguing muscle defects. ***(Am J Pathol 2007, 170:316–333; DOI: 10.2353/ajpath.2007.060687)***

Tubular aggregates (TAs) were first described by Engel in 1964 as granular "crystal-like" inclusions in skeletal muscle sections, associated with mitochondrial aggregates.[1] Indeed, TAs are very peculiar structures, found in the skeletal muscle of patients with a wide range of neuromuscular disorders. They consist of very densely packed tubules located between the myofibrils and beneath the sarcolemma and arranged in such an organized fashion to resemble crystal formation.[2,3] Although TA formation is the primary symptom in a very rare inherited myopathy, tubular aggregate myopathy,[4–6] more often TAs are a relatively nonspecific feature of numerous human skeletal muscle pathological conditions, including sporadic limb girdle weakness,[7] familial myasthenia gravis,[8, 9] exercise-induced cramps,[10] periodic paralysis,[11] and gyrate atrophy of the choroid and retina.[12]

The mechanisms underlying the formation of TAs and their functional significance in skeletal muscle remains unknown. As these structures stain positive with the nicotinamide-adenine dinucleotide (NADH)-tetrazolium reductase reaction, they were initially believed to originate from mitochondria or to consist of mitochondrial aggregates. However, work by several groups has now shown that tubular aggregates arise from the terminal cisternae or longitudinal components of the sarcoplasmic reticulum.[13] Interestingly, a recent study has again advocated that a mitochondrial component may be involved in the formation of tubular aggregates,[14] clearly illustrating that

Supported by grants from the National Institutes of Health, the Muscular Dystrophy Association, and the American Heart Association (all to M.P.L.).

Accepted for publication September 20, 2006.

Supplemental material for this article can be found on *http://ajp.amjpathol.org*.

Address reprint requests to Dr. Michael P. Lisanti, Department of Cancer Biology, Kimmel Cancer Center, Bluemle Life Sciences Building, Room 933, 233 S. 10th Street, Philadelphia, PA 19107. E-mail: michael.lisanti@jefferson.edu.

the pathophysiology of TA formation remains controversial. In addition, several reports have demonstrated that tubular aggregate formation is often found associated with the abnormal proliferation and accumulation of mitochondria in myopathic skeletal muscle fibers.

Unfortunately, the study of the molecular basis of TA formation has been hampered by the lack of a genetic mouse model, demonstrating TA formation as a primary defect. The natural occurrence of TAs in the skeletal muscle was detected in several different mouse strains, including the senescence-accelerated mouse,[15] a dystrophic mouse strain,[16] and the $MLR^{+/+}$ substrain mouse.[17] In addition, Agbulut et al have reported that TA formation occurs in all inbred mouse strains they examined, in an age- and sex-dependent manner.[18] Tubular aggregates were observed only in male mice, with their incidence increasing with age.

In this article, we describe the presence of tubular aggregates and mitochondrial proliferation/aggregation in the skeletal muscle fibers of a mouse model that harbors the genetic ablation of the caveolin (Cav)-2 gene. Our results suggest that loss of Cav-2 function may represent a novel underlying cause for tubular aggregate formation.

Materials and Methods

Antibodies

Antibodies and their sources were as follows. Anti-Cav-1 polyclonal antibody (pAb) (N-20), anti-mitochondrial-specific creatine kinase (sMtCK) pAb (C-18), anti-MCK pAb (N-13), and anti-dihydropyridine receptor (DHPR) pAb (N-19) were from Santa Cruz Biotechnology (Santa Cruz, CA). Anti-Cav-2 monoclonal antibody (mAb) (clone 65) and anti-Cav-3 mAb (clone 26) were generous gifts of Roberto Campos-Gonzalez, BD-Pharmingen (San Diego, CA). Anti-GRP-78 pAb, anti-sarcoplasmic and endoplasmic reticulum calcium ATPase-1 (SERCA-1) mAb, and anti-SERCA-2 mAb were from Affinity Bioreagents (Golden, CO). Anti-calsequestrin mAb and anti-M-cadherin mAb were from BD-Pharmingen. Anti-actin mAb was from Sigma (St. Louis, MO). Anti-heat shock protein 60-kd (HSP-60) pAb was from Stressgen (Ann Arbor, MI). Anti-dicarboxylate carrier (DIC) pAb was the gift of Philipp E. Scherer (Albert Einstein College of Medicine, Bronx, NY).

Animal Studies

All animals were housed and maintained in a pathogen-free environment/barrier facility at the Institute for Animal Studies at the Albert Einstein College of Medicine and at Thomas Jefferson University, under the National Institutes of Health (NIH) guidelines. Cav-1-, Cav-2-, and Cav-3-deficient mice were generated, as we previously described,[19–21] and were in the C57Bl/6 genetic background. $INK4a^{(-/-)}$ mice (in the C57Bl/6 background) were used for the generation of the myoblasts and were the generous gift of Dr. Ron DePinho (Harvard Medical School, Boston, MA).

Myoblast Cell Line Generation

One-month-old male $INK4a^{(-/-)}$ mice were sacrificed, and the skeletal muscle was carefully removed under sterile conditions, cleaned of surrounding tissue, and washed in Hanks' balanced salt solution (HBSS) supplemented with 10 mmol/L 4-(2-hydroxyethyl)-1-piperazineethanesulfonic acid (HEPES). Tissue samples were minced and placed in a 10-ml solution of HBSS-HEPES containing 2 mg/ml collagenase type I (Worthington Biochemical, Freehold, NJ) and agitated for 60 minutes at ~175 rpm at 37°C. Then, the samples were gently centrifuged, and the supernatant was removed by aspiration. Cell pellets were washed twice by centrifugation and plated on 10-cm plastic dishes (Corning, Acton, MA) in Dulbecco's modified Eagle's medium containing glutamine, antibiotics (penicillin and streptomycin), and 10% fetal calf serum. The cells were allowed to attach for 24 hours, after which time they were passed and replated. Two days after confluence, the cells were noted to begin differentiating into myotubes. After ~4 days in conditioned media, the myotubes began spontaneously contracting.

Electron Microscopy

Male mice from the different genotypes were sacrificed, and the gastrocnemius muscle was removed. Tissue samples were fixed with 2% paraformaldehyde and 2.5% glutaraldehyde in 0.1 mol/L cacodylate buffer, postfixed with OsO_4, *en bloc*-stained with uranyl acetate, and embedded in epoxy resin. Ultrathin sections were examined with a JEOL 1200 EX transmission electron microscope (Tokyo, Japan). Cells from the myoblast cell line were processed for electron microscopy in a similar manner as the tissue samples, except that cells were pelleted before embedding and sectioning.

Immunofluorescence

Male mice from the different genotypes were sacrificed, and the gastrocnemius muscle was removed. Tissue samples were fixed in 4% paraformaldehyde overnight, followed by extensive washing in phosphate-buffered saline (PBS) and cryoprotected in 30% sucrose overnight. The samples were then placed in OCT mounting media (Tissue-Tek; Electron Microscopy Sciences, Hatfield, PA) and snap-frozen in liquid nitrogen-cooled isopentane. Five-micron-thick sections were cut and placed on slides, allowed to adhere overnight, and stored at −80°C. Slides were warmed to room temperature, washed with PBS to remove OCT, and incubated with a blocking solution (PBS, 2% goat serum, 1% bovine serum albumin, and 0.1% Triton X-100) for 20 minutes. Then, sections were incubated with primary antibodies for 1 hour at room temperature at the dilution suggested by the manufacturer. The sections were washed in PBS and incubated in

the appropriate secondary antibody (Jackson Laboratories) at a dilution of 1:1000 for 30 minutes. After washing, sections were mounted with Slowfade anti-fade reagent (Molecular Probes, Eugene, OR) and examined under an Olympus IX70 inverted microscope (Tokyo, Japan). Images were acquired using a Sensicam QE cooled CCD camera.

Quantification of Tubular Aggregates Size, Muscle Fibers Areas, and Sarcoplasmic Reticulum Volume

Images of cross sections of gastrocnemius muscle were acquired at ×20 magnification. The measurement of tubular aggregate size was performed on cross-sections stained with the SERCA-1 antibody. The measurement of muscle fiber area was performed on cross-sections stained with Cav-3 antibody. Electron micrographs were used to measure the volume of the sarcoplasmic reticulum. Images were analyzed using NIH Image J software, and raw data were imported into Microsoft Excel for statistical analysis and graphic representation. Importantly, sampling for tissue sections and electron microscopy was performed in a blinded fashion.

Immunoblot Analysis

Male mice from the different genotypes were sacrificed, and the gastrocnemius muscle was isolated. Skeletal muscle samples were homogenized in lysis buffer [10 mmol/L Tris, pH 7.4, 1% sodium dodecyl sulfate (SDS), and 1 mmol/L orthovanadate] containing protease inhibitors (Roche Diagnostics, Indianapolis, IN) and centrifuged at 13,000 × *g* for 10 minutes to remove insoluble debris. Protein concentrations were determined using bicinchoninic acid reagent (Pierce, Rockford, IL). Tissue lysates (35 μg) were separated by SDS-polyacrylamide gel electrophoresis (10% acrylamide) and transferred to nitrocellulose. Membranes were subjected to immunoblot analysis as previously described,[22] except primary antibody concentrations were as suggested by the company.

Muscle Regeneration

Age-matched 8-month-old male mice from the different genotypes were anesthetized using ketamine and xylazine. The hair from the lower legs was removed. A small horizontal incision was made to expose the lower portion of the gastrocnemius muscle just above the site of tendon insertion. Ten μl of notexin (Sigma) was injected into the length of the right gastrocnemius muscle at a concentration of 50 μg/ml using a 25-μl Hamilton syringe (Reno, NV). The wound was closed with a surgical staple. The left leg was similarly treated, except 10 μl of saline was injected as a control. The site of injection was marked by dipping the tip of the needle into India ink before injection. Three and 7 days after injection, animals were sacrificed, and muscles were harvested, fixed, and processed for cryosectioning. Fifteen-micron-thick sections were prepared from various regions within the muscle and subjected to immunofluorescence analysis.

Mithocondrial Examination

Morphological analysis of skeletal muscle and staining for cytochrome *c* oxidase (COX), NADH, and succinate dehydrogenase (SDH) activities were performed, as previously described.[23] Biochemical analysis of respiratory chain enzyme activities and citrate synthesis in skeletal muscle homogenates was performed as described.[24]

Results

Cav-1 and Cav-2 Are Down-Regulated during Skeletal Muscle Differentiation and Myotube Formation

Cav-3 is highly expressed at the sarcolemma of mature skeletal muscle fibers, whereas Cav-1 and -2 are clearly absent in adult skeletal muscle fibers.[6] Nonetheless, Cav-1 and -2 are thought to be expressed in undifferentiated myotube precursor cells (such as satellite cells and myoblasts). As such, it has been hypothesized that Cav-3 functionally replaces Cav-1 and -2 in fully differentiated adult skeletal muscle fibers. In support of this hypothesis, undifferentiated C2C12 cells, a mouse-derived skeletal muscle cell line, co-express Cav-1 and -2 but fail to express Cav-3. Interestingly, upon differentiation of C2C12 from myoblasts to myotubes, Cav-3 expression increases, but Cav-1 and -2 levels remain unchanged, probably because differentiated C2C12 myotubes retain an embryonic phenotype. Thus, it has never been formally demonstrated that Cav-1 and -2 undergo down-regulation during myoblast differentiation.

To address this issue, we examined the expression levels of caveolin isoforms during skeletal muscle differentiation, using primary cultures of myoblasts derived from INK4a$^{(-/-)}$-null mice. Importantly, loss of the INK4a cell cycle regulatory proteins (p16 and p19ARF) is sufficient to confer immortalization but not transformation.[25] Thus, we used INK4a$^{(-/-)}$-null skeletal muscle to develop a novel myoblast cell line. We first attempted to evaluate whether this novel myoblast cell line can recapitulate the differentiation process of skeletal muscle *in vitro*. Under the appropriate conditions, we observe that INK4a$^{(-/-)}$ myoblasts undergo differentiation and spontaneously form myotubes—approximately 2 to 3 days after they reach ~100% confluence (Figure 1A). Remarkably, when the cell culture dish was gently agitated, many of the myotubes underwent spontaneous contractions or appeared to "beat" (cyclical contractions). We also examined the ultrastructure of these INK4a$^{(-/-)}$ myotubes by transmission electron microscopy. Interestingly, they contain numerous caveolae at the sarcolemma (not shown) and show the development of sarcomeres, with clear Z-lines (Figure 1B). Additional evidence for sarcomeric organization within these myotubes was obtained

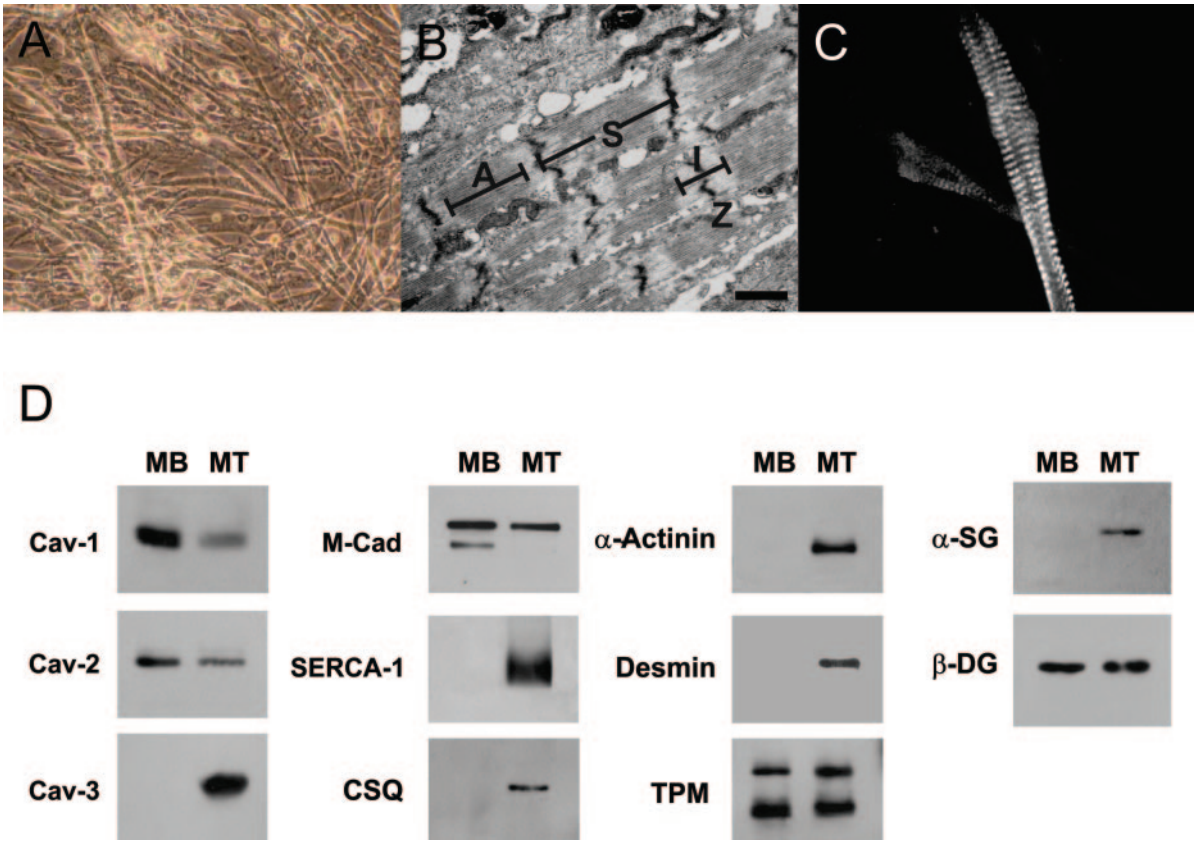

Figure 1. Cav-1 and Cav-2 are down-regulated during skeletal muscle differentiation and myotube formation in primary cultures of INK4a$^{(-/-)}$ skeletal muscle myoblasts. To directly evaluate Cav-1 and Cav-2 expression levels during skeletal muscle differentiation, we derived and characterized a novel INK4a$^{(-/-)}$ skeletal muscle cell line. **A:** INK4a$^{(-/-)}$ skeletal muscle myoblasts undergo spontaneous differentiation and form myotubes approximately 2 to 3 days after they reach ~100% confluence. A phase-contrast image of these differentiated myotubes is shown. **B:** Ultrastructural analysis of INK4a (−/−) myotubes by transmission electron microscopy. Note the presence of sarcomeres (S). Z, Z-line; A, A-band; I, I-band. **C:** Myotubes were immunostained with an antibody that recognizes the sarcomeric myosin heavy chain of vertebrate muscle (mAb MF20). Note the striated pattern, characteristic of differentiated skeletal muscle myotubes. **D:** INK4a$^{(-/-)}$ myoblasts undergo differentiation and express muscle-specific marker proteins. Note that Cav-1, Cav-2, and M-cadherin are predominantly expressed in the undifferentiated cells, with their expression levels decreasing during differentiation. Conversely, markers of differentiated skeletal muscle cells, such as Cav-3, SERCA-1, calsequestrin (CSQ), α-actinin, desmin, and α-sarcoglycan (α-SG), are elevated during differentiation. Significantly, other proteins seem to be expressed equally in undifferentiated and differentiated INK4a$^{(-/-)}$ skeletal muscle cells, namely tropomyosin (TPM) and β-dystroglycan (β-DG). Each lane contains an equal amount of total protein. MB, myoblasts (undifferentiated); MT, myotubes (differentiated). Scale bar = 1 μm.

by immunostaining with an antibody that specifically recognizes the sarcomeric myosin heavy chain of vertebrates (mAb MF20). Interestingly, myosin heavy chain exhibited a striated staining pattern in INK4a$^{(-/-)}$ myotubes (Figure 1C).

Western blot analysis independently confirmed that, upon differentiation, INK4a$^{(-/-)}$ myotubes express a variety of muscle-specific marker proteins (Figure 1D). More specifically, during myotube formation, we detected induction of expression of Cav-3, SERCA-1, calsequestrin, α-actinin, desmin, and α-sarcoglycan. In contrast, M-cadherin, a marker of satellite cells, Cav-1, and Cav-2 were all down-regulated during muscle cell differentiation. Finally, the levels of tropomyosin and β-dystroglycan remained unchanged.

These results demonstrate that the novel INK4a$^{(-/-)}$ myoblast cell line represents a valid system for studying the molecular events that occur during skeletal muscle differentiation. In addition, these findings show that skeletal muscle differentiation involves Cav-1 and Cav-2 down-regulation and suggest that the three caveolin isoforms are transiently co-expressed and may interact during myotube differentiation.

Cav-2-Deficient Mice Show Tubular Aggregate Formation in Skeletal Muscle

To assess the physiological role of non-muscle caveolins in skeletal muscle, we next decided to use an *in vivo* molecular genetic approach. Based on the observations that Cav-1 and Cav-2 expression is elevated in myogenic precursor cells and tightly regulated during muscle differentiation, we would predict that loss of Cav-1 and/or Cav-2 may induce significant disturbances in skeletal muscle.

We first analyzed the effect of a Cav-2 deficiency on skeletal muscle. To this end, we examined by electron microscopy skeletal muscle from 3-month-old Cav-2$^{(-/-)}$-null mice. It was surprising to observe that Cav-2-deficient skeletal muscle displayed profoundly perturbed skeletal muscle morphology and exhibited tubular aggregate forma-

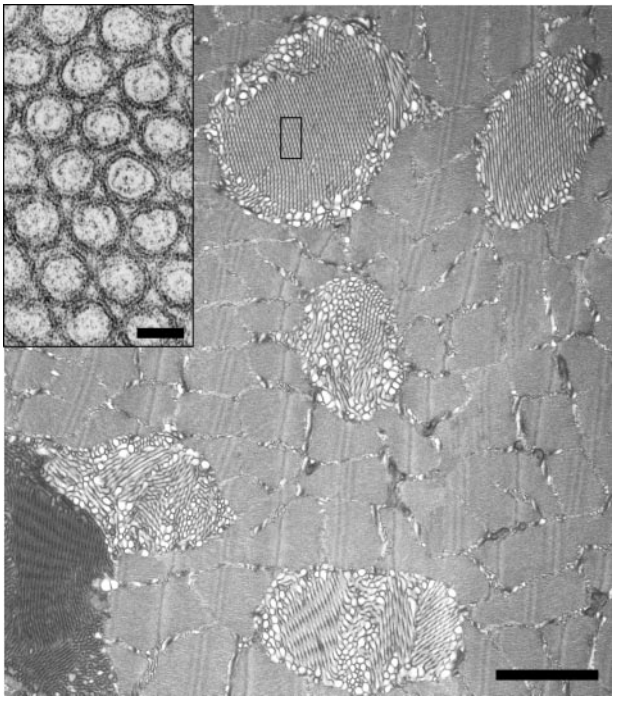

Figure 2. Cav-2-deficient skeletal muscle fibers display tubular aggregate formation. Low-magnification electron micrograph of skeletal muscle from 3-month-old Cav-2-deficient mice. Note the multiple examples of tubular aggregate formation. A high-magnification **inset** reveals the crystalline-like organization of tubular aggregates. Scale bar for low-magnification image = 1 μm; scale bar in insert = 50 nm.

tion. Figure 2 shows that the overall size, shape, and organizational appearance of tubular aggregates can vary widely. Interestingly, when the tubular aggregates occurred in a highly organized fashion, the lumen of the tubules contained an electron-dense core that also appears to be extremely ordered (Figure 2, inset). However, we could not detect any tubular aggregates in Cav-2-deficient pups (not shown), consistent with the idea that tubular aggregate formation is age-dependent. Importantly, only male mice were affected. In addition, there did not seem to be a relationship between the tubular aggregates and the location of the sarcoplasmic reticulum (SR) in our electron micrographs.

Previous studies have suggested that TA formation is a nonspecific muscle phenomenon of aged inbred male mice.[18] To begin to evaluate the specificity of our findings, we next examined by electron microscopy skeletal muscle derived from 8-month-old male wild-type (WT), Cav-1 knockout (KO), Cav-2 KO, and Cav-3 KO mice. Interestingly, TA formation was detected only in skeletal muscle isolated from Cav-1- and Cav-2-deficient mice (Figure 3) but not from Cav-3-deficient mice. These results suggest that TA formation is restricted to Cav-1- and Cav-2-null skeletal muscle. In addition, because of the nature of the interaction between Cav-1 and Cav-2, we can attribute this phenotype to Cav-2 loss and not to Cav-1 deficiency. Previous results have demonstrated that in the absence of Cav-1, Cav-2 expression is almost completely abolished. As such, Cav-1-deficient mice are deficient in both Cav-1 and Cav-2.[19] However, Cav-2 is not needed for the proper functioning and localization of Cav-1, and the levels of Cav-1 protein are not affected in Cav-2-deficient mice[20] (see also Figure 6B). In addition, we noticed that tubular aggregate formation appears to be restricted to skeletal muscle, since no tubular aggregates were detected in either cardiac or smooth muscle in any of the caveolin knock-out mice examined (data not shown).

Cav-2 Deficiency Does Not Affect Caveolae Formation and Proper Cav-3 Localization

We next evaluated whether loss of Cav-2 induces TA formation, secondary to alterations either in caveolae formation or in the expression levels of the muscle-specific caveolin isoform Cav-3. To detect caveolae formation, we examined high-magnification electron micrographs of WT and Cav-2-deficient skeletal muscle. Figure 4A shows the presence of numerous caveolae at the plasma membrane of skeletal muscle fibers from both WT and Cav-2-deficient mice, suggesting that loss of Cav-2 does not affect caveolae formation. In addition, Figure 4A shows that a tubular aggregate structure is clearly visible in the micrograph of the Cav-2-deficient skeletal muscle in close proximity to the plasma membrane. To assess whether loss of Cav-2 alters the expression or distribution of Cav-3, in some way resulting in the development of the tubular aggregates, cryosections from WT and Cav-2-deficient skeletal muscle were subjected to immunofluorescence analysis with an antibody directed against Cav-3. Figure 4B shows that the relative staining intensity and distribution of Cav-3 is unchanged in Cav-2-deficient mice compared with WT controls. In addition, the same sections were double-immunostained with an antibody against SERCA-1, a known marker of tubular aggregates. Figure 4B demonstrates the presence of numerous tubular aggregates in the skeletal muscle fibers from the Cav-2-deficient mice. However, we detected few, if any, SERCA-1-positive fibers in WT controls (Figure 4B). These data confirm that the development of tubular aggregates is due to the loss of Cav-2 in skeletal muscle fibers and does not correlate with impairment of caveolae formation and/or changes in the expression profile of Cav-3.

The Frequency and Size of Tubular Aggregates Is Significantly Increased in Cav-2-Deficient Skeletal Muscle

The occurrence of TA formation in male WT mice has previously been reported as an age-related phenomenon.[18] Consistent with these findings, during the course of our study we were also able to identify the presence of tubular aggregates in WT mice. However, the frequency and the size of individual aggregates appeared strikingly increased in Cav-2-deficient skeletal muscle compared with age-matched WT controls. To quantify these differences, skeletal muscle sections from three different 8-month-old WT and Cav-2-defi-

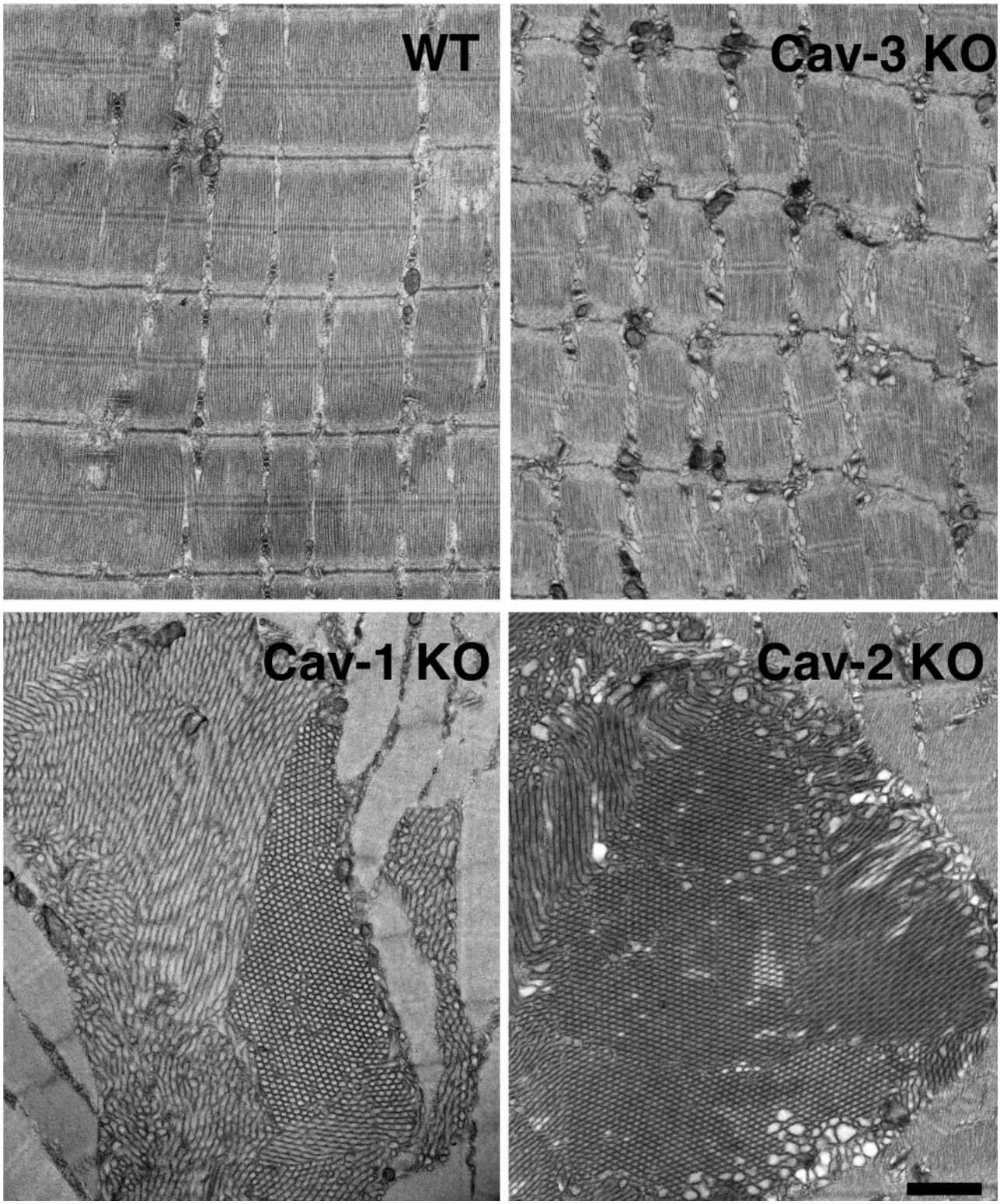

Figure 3. Tubular aggregate formation occurs in Cav-1- and Cav-2-deficient mice but not in Cav-3-deficient mice. Electron microscopic examination of skeletal muscles from 8-month-old WT, Cav-1, Cav-2, and Cav-3 KO mice. Note that skeletal muscles from Cav-1- and Cav-2-deficient mice contain tubular aggregates. However, WT and Cav-3 KO mice do not display any tubular aggregate formation. WT skeletal muscle exhibits normal cyto-architecture and sarcomere organization, whereas, as expected, Cav-3-deficient mice display mild disorganization. Scale bar in Cav-2 KO panel = 500 nm and applies to all four images.

cient mice were stained with a SERCA-1 antibody to visualize TA formation (Figure 5A). SERCA-1 is the best known marker for the detection of TA formation by immunofluorescence. (However, we cannot completely exclude the possibility that we are also detecting expanded SR.)

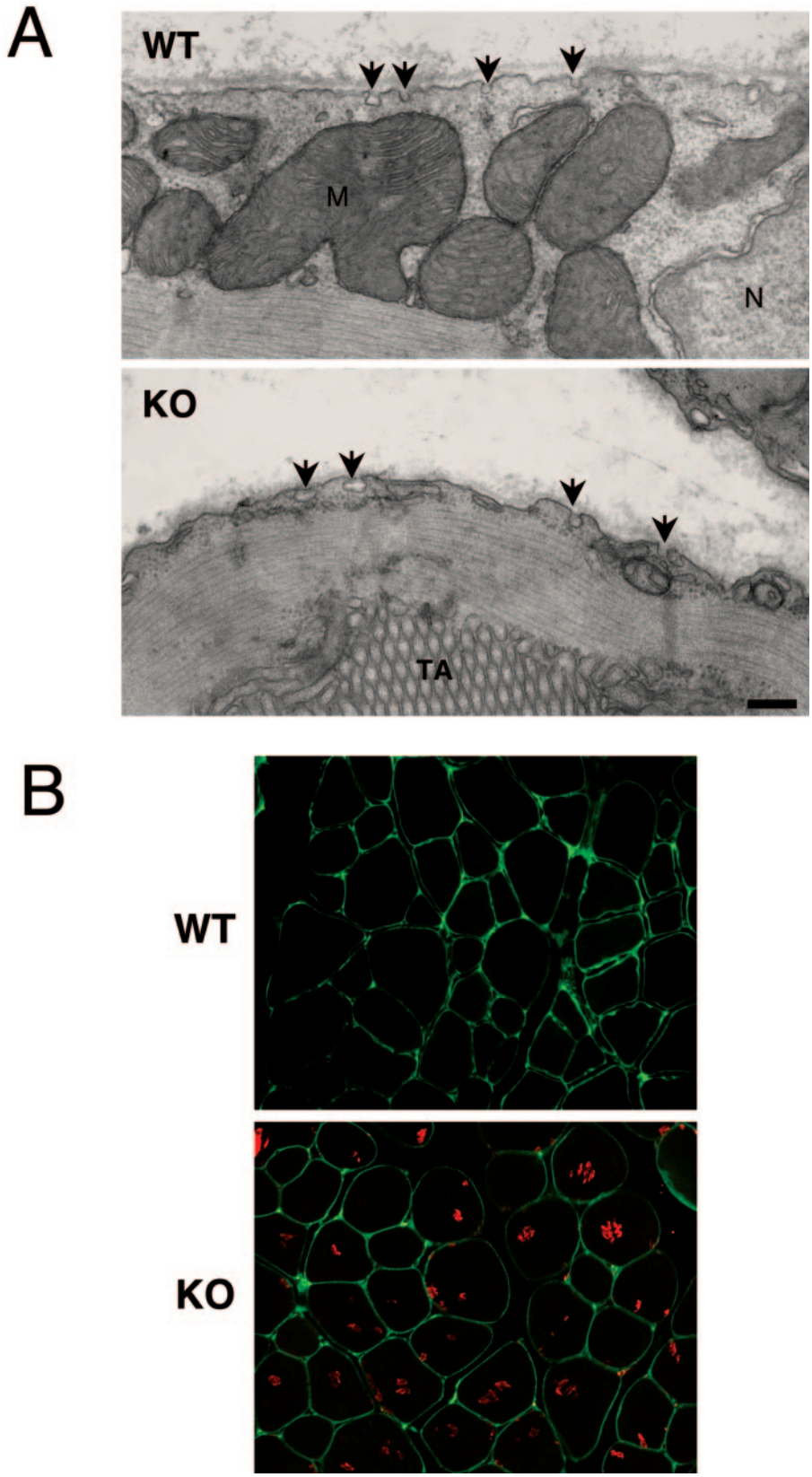

Figure 4. Cav-2-deficient skeletal muscle fibers retain the ability to form caveolae and exhibit normal Cav-3 levels and distribution. **A:** Electron micrographs demonstrate that both WT and Cav-2 KO skeletal muscle have abundant caveolae (**arrows**) at the plasma membrane. Note the presence of a tubular aggregate (TA) in the Cav-2 KO micrograph. M, mitochondria. N, nucleus. Scale bar in KO = 250 nm and applies to both images. **B:** Cav-3 (green) is localized at the plasma membrane in WT and Cav-2-deficient mice skeletal muscle. Staining with an antibody to SERCA-1 (red) reveals extensive tubular aggregate formation in Cav-2 deficient but not in WT skeletal muscle fibers.

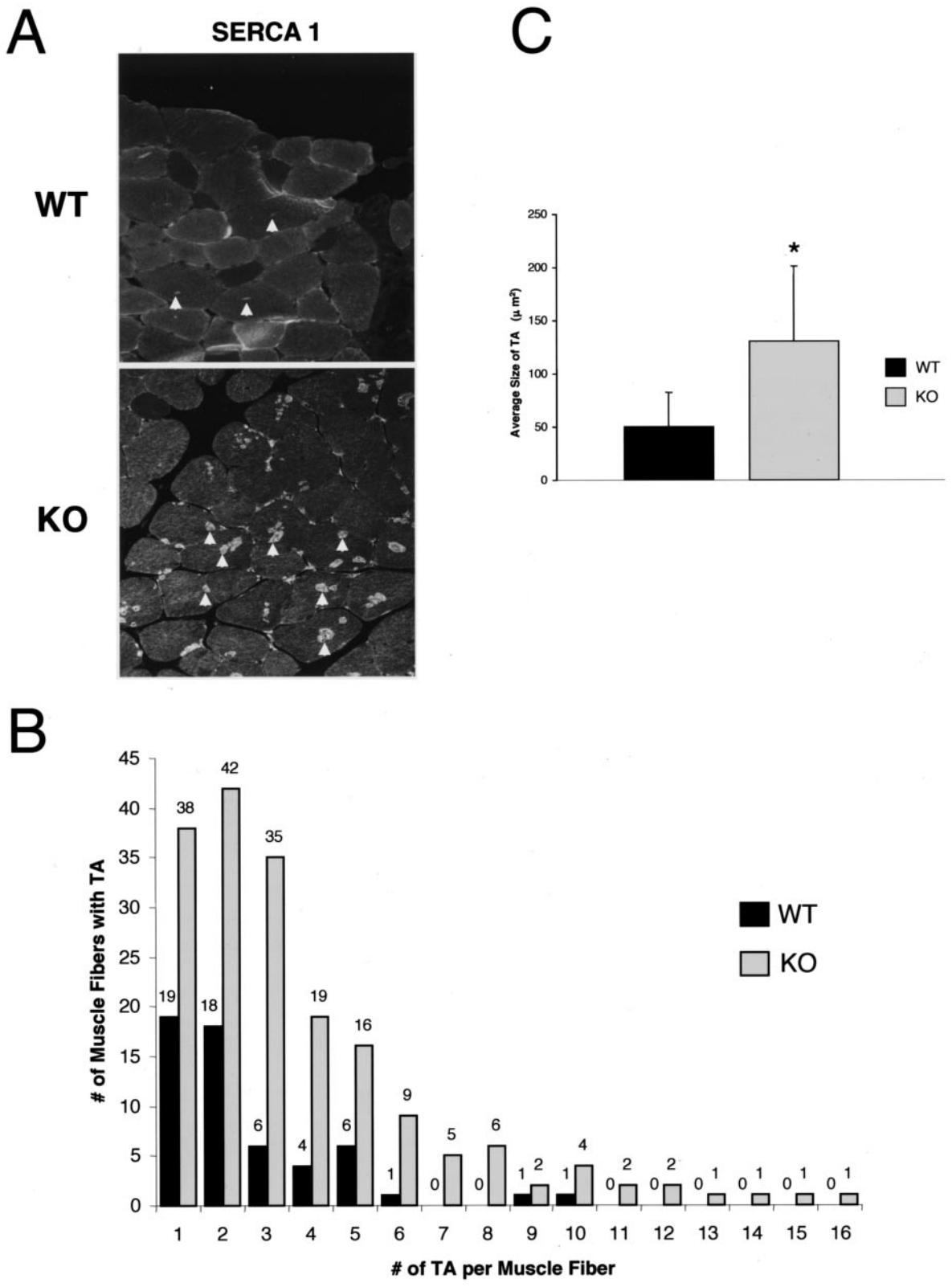

Figure 5. The frequency and size of tubular aggregates are significantly increased in Cav-2-deficient skeletal muscle. **A:** Skeletal muscle cross-sections from 8-month-old WT and Cav-2-deficient mice were labeled with a SERCA-1 antibody. Note the increase in the number and size of tubular aggregates (**arrowheads**) in Cav-2 KO mice compared with their WT counterparts. **B:** Quantitation of the frequency of tubular aggregate formation in WT and Cav-2 KO sections, which were stained with a marker for tubular aggregates, SERCA-1. The frequency was determined by plotting the number of tubular aggregates per individual muscle fiber versus the number of muscle fibers with tubular aggregates. Note that Cav-2-deficient myofibers exhibit more fibers with tubular aggregates and more tubular aggregates per individual muscle fiber, suggesting that Cav-2-null mice are more likely to develop tubular aggregates than age-matched WT mice. **C:** The average size of tubular aggregates in Cav-2 KO mice is significantly increased compared with age-matched WT mice. The average size of TAs in WT muscle fibers is 39.8 μm^2, whereas the average size of TAs in the Cav-2-deficient muscle cells is 130.6 μm^2 ($^*P < 0.005$).

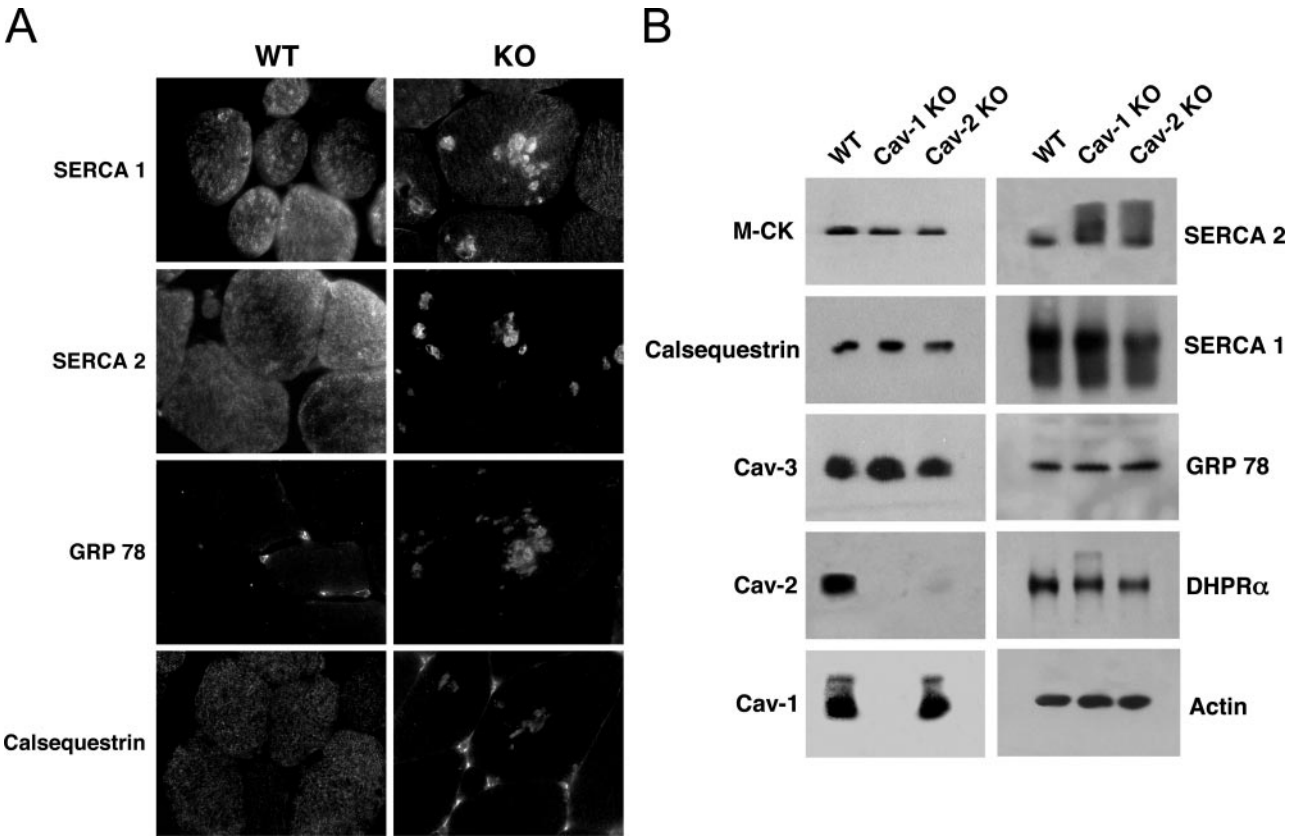

Figure 6. Distribution and expression profile of sarcoplasmic-reticulum-marker proteins. **A:** Immunofluorescence analysis of several SR resident proteins, including SERCA-1, SERCA-2, GRP78, and calsequestrin. Note that tubular aggregates consistently express SR resident proteins. Interestingly, the localization of calsequestrin is altered in Cav-2-deficient skeletal muscles, as compared with WT controls. Calsequestrin seems localized to TAs, as well as at the plasma membrane in Cav-2-deficient myofibers, whereas it is localized to the SR in WT controls. **B:** Western blot analysis of WT and Cav-2 KO skeletal muscles with antibodies against SR resident proteins (SERCA-1, SERCA-2, GRP78, and calsequestrin), muscle-specific proteins, and caveolin isoforms. Note that the endogenous expression levels of certain SR resident proteins, including SERCA-1, GRP78, and calsequestrin, are unchanged in Cav-2-deficient skeletal muscle compared with WT controls, suggesting that these proteins are redistributed to TAs within the myofibers. However, SERCA-2 is up-regulated in Cav-2 KO samples, due to the fact that, besides the expected expression in type I muscle fibers, SERCA-2 is abnormally expressed in TAs in type II fibers (data not shown). In addition, the expression levels of a T-tubule-specific marker, DHPRα, and of the cytoplasmic M-CK are not changed in Cav-2 KO skeletal muscle. As expected, loss of Cav-2 does not affect Cav-3 expression levels. Interestingly, Cav-2-deficient skeletal muscles display normal expression levels of Cav-1, whereas Cav-1 deficiency abrogates almost completely Cav-2 expression. Equal loading was assessed by Western blot with actin.

Then, the number and the size of individual aggregates were scored in over 300 individual skeletal muscle fibers (Figure 5, B and C). Figure 5B shows the distribution of the number of TA in WT and Cav-2-deficient skeletal muscle. Of the 300 WT fibers examined, only 17% contained any aggregates, and two-thirds of these had only one or two aggregates per fiber. On the contrary, over 56% of the Cav-2-deficient fibers contained aggregates and over half of those had three or more aggregates per fiber, with 12 individual fibers containing 10 or more individual aggregates.

In addition, Figure 5C shows that the size of individual aggregates was increased ~2.6-fold in Cav-2-deficient fibers compared with WT fibers. Interestingly, at 3 months of age, WT skeletal muscle contained no detectable TAs, whereas Cav-2-deficient skeletal muscle contained numerous tubular aggregates at this age. These data indicate that the onset of tubular aggregate formation is greatly accelerated in Cav-2-deficient mice compared with WT animals.

Expression Levels and Distribution of Sarcoplasmic Reticulum Markers

The pathophysiology of TA formation still remains controversial. Multiple lines of evidence strongly suggest that TAs originate from the SR, whereas independent researchers advocate for additional mitochondrial components.[13,14] To gain insights into this issue, we analyzed the distribution of resident markers of the SR in skeletal muscle sections from 8-month-old age-matched WT and Cav-2-deficient mice. We examined the distribution of two membrane-bound enzymes, SERCA-1 and SERCA-2, of an intraluminal calcium-binding protein, calsequestrin, and, finally, of an SR-specific heat-shock protein, GRP78. Figure 6 shows that all four SR-specific markers (SERCA-1, SERCA-2, GRP78, and calsequestrin) localized to tubular aggregates within the muscle fibers of Cav-2-deficient mice, suggestive of a strong SR component in tubular aggregate formation. Interestingly, the

localization of calsequestrin is significantly altered in the skeletal muscle of Cav-2-deficient mice compared with WT counterparts. Figure 6 shows that calsequestrin displayed diffuse cytoplasmic staining, consistent with SR localization in WT muscle fibers, whereas it localized to TAs as well as to the plasma membrane in Cav-2-deficient myofibers.

We next asked whether the presence of TAs would change the expression profile of muscle-specific proteins, including SR resident molecules. For this purpose, skeletal muscle samples from 8-month-old age-matched WT, Cav-1-, and Cav-2-deficient mice were subjected to Western blot analysis with antibodies against 1) SR resident proteins SERCA-1, SERCA-2, GRP78, and calsequestrin; 2) the T-tubule-specific marker dihydropyridine receptor-1α (DHPRα); 3) a cytoplasmic muscle enzyme, muscle creatine kinase (M-CK); and 4) the caveolin isoforms.

Figure 6B shows that SERCA-2 levels appeared increased in Cav-1- and Cav-2-deficient skeletal muscle. These results are consistent with the immunofluorescence data (not shown), revealing that Cav-2-null fibers express SERCA-2 in type I fibers, as expected, but also in TAs in type II fibers (Supplemental Figure 1, see *http://ajp.amjpathol.org*). The fact that the expression levels of other SR proteins is not changed in WT and Cav-2-deficient muscle suggests that the presence of TA does not result in an increase in SR proteins but rather induces the relocation of a certain percentage of the endogenous proteins. In addition, we could not detect changes in the expression levels of markers of the cytoplasm M-CK and of the T-tubule system DHPRα. Moreover, Cav-3 expression was unaltered in Cav-1- and Cav-2-deficient muscle. Finally, we demonstrate that loss of Cav-2 does not affect Cav-1 expression in muscle, whereas loss of Cav-1 abrogates Cav-2 expression.

The Sarcoplasmic Reticulum Is Dilated in Cav-2-Deficient Skeletal Muscle

To further explore the nature of TA formation, and to corroborate the idea that TAs originate from abnormal dilatation and proliferation of the SR, we evaluated, by electron microscopy, the status of the SR in skeletal muscle samples from 8-month-old WT and Cav-2 KO mice. Figure 7A shows representative micrographs to illustrate that the SR tubules appear significantly dilated in Cav-2-deficient skeletal muscle compared with their WT counterparts. Note the substantial increase in tubule number and volume in Cav-2-null skeletal muscle.

To quantify the SR increase, we calculated the percentage of area occupied by the SR versus the total muscle area. To this end, we measured both the SR area and the overall muscle area in numerous electron micrographs of skeletal muscle from newborn, 3-month-old, and 8-month-old WT and Cav-2-null mice. For comparison, we also monitored the SR area in skeletal muscle from 8-month-old Cav-1-null mice. Figure 7B reveals a significant increase in the area occupied by the SR in 3- and 8-month-old Cav-2-deficient skeletal muscle compared with WT controls. More specifically, at 3 months of age, the area occupied by the SR increased more than twice in Cav-2-deficient muscle, with 12.9% of the total muscle area being occupied by SR tubules in Cav-2-null myofibers versus 5.8% in WT controls. A similar pattern was evident at 8 months, with 10.1% of total muscle area occupied by the SR in Cav-2 KO mice and 4.7% in their WT counterparts. Interestingly, at 8 months, Cav-1-deficient mice displayed a phenotype similar to Cav-2-deficient mice, with 9.8% of the total muscle area being occupied by SR tubules in Cav-1-null myofibers. However, Cav-2-deficient pups displayed only a small, not statistically different, increase in the muscle area occupied by the SR. It is interesting to note the correlation between the onset of the tubular aggregate formation and of sarcoplasmic reticulum dilation. In fact, the tubular aggregates could be detected in mice at 3 months, a time when SR dilatation seems to be at its highest, but not in newborns, when SR dilatation is not dramatically different between WT and Cav-2-deficient mice, suggesting that SR enlargement may precede TA formation.

Cav-2-Deficient Skeletal Muscle Contains Large Mitochondrial Aggregates

During our detailed examination of electron micrographs, we noticed other interesting changes in Cav-2-deficient skeletal muscle. For example, Figure 8A reveals large mitochondrial aggregates in 3- and 8-month-old Cav-2 KO mice. These aggregates occurred in two distinct patterns. Panels A and B illustrate examples of an amorphous mass of mitochondria tightly packed together, whereas panels C and D are representative of more organized circular assemblies, containing numerous mitochondria, as well as other vacuolar structures. Mitochondrial aggregates were observed within the muscle fiber and, in many instances, disrupted the organization of the sarcomere itself (see panels A and C).

To deepen our understanding of the abnormal mitochondrial aggregation of Cav-2-deficient mice, skeletal muscle samples from 8-month-old WT, Cav-1-, and Cav-2-deficient muscle were subjected to Western blot analysis with mitochondrial-specific markers, including sMtCK, DIC, HSP-60, and voltage-dependent anion channel (VDAC). Figure 8B shows that the expression levels of two mitochondrial markers, DIC and HSP-60, were increased in Cav-1- and Cav-2-deficient muscle compared with their WT counterparts. Similarly to the tubular aggregates and dilated SR, the mitochondrial aggregates could be detected in 3-month-old Cav-2 KO mice but not in newborn pups (data not shown).

To evaluate further the mitochondrial proliferation of Cav-2-deficient mice, skeletal muscle sections from 8-month-old WT and Cav-2 KO mice were subjected to histochemical examination with mitochondrial-specific enzymatic stains, including COX (Figure 9A), NADH, SDH, and trichrome staining (Supplemental Figure 1,

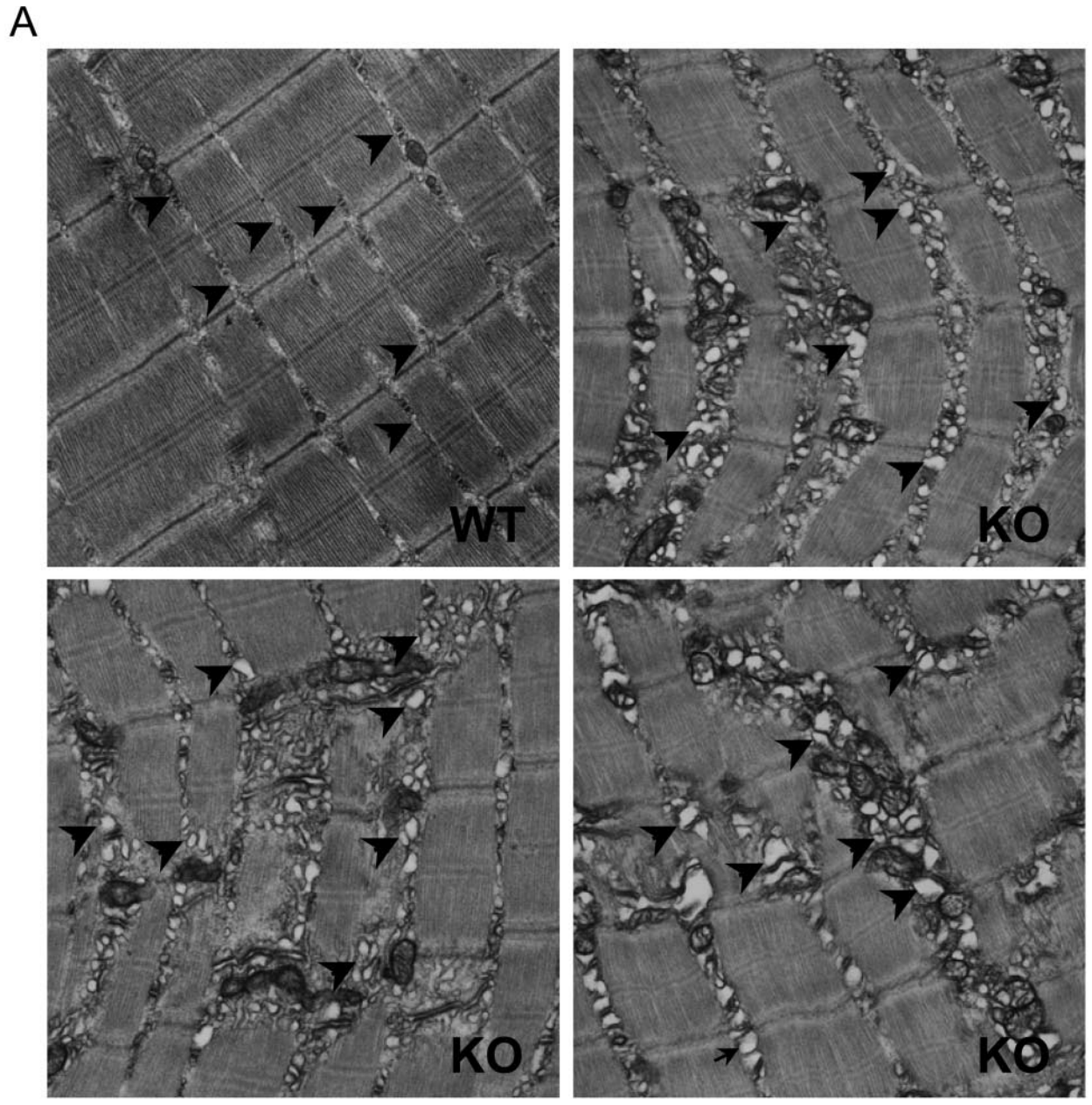

Figure 7. Loss of Cav-2 disrupts the organization and volume of the sarcoplasmic reticulum in skeletal muscle. **A:** Note that the SR of skeletal muscle from Cav-2-deficient mice is swollen compared with WT controls. **Arrowheads** illustrate numerous examples of the enlarged SR in Cav-2 KO mice. **B:** The overall skeletal muscle area occupied by the SR (E-C coupling system) in Cav-2-deficient mice is significantly increased at both 3 and 8 months of age compared with WT controls. At three months of age, the percentage of skeletal muscle occupied by the SR in Cav-2-null mice was 12.9 versus 5.9% in WT controls ($^*P < 0.005$). Interestingly, 8-month-old Cav-1-deficient mice have a similar increase in SR volume as Cav-2-deficient mice. At 8 months of age, the percent area occupied by the SR in WT skeletal muscle was 4.7%, compared with 9.8 and 9.6% for the Cav-2- and Cav-1-deficient skeletal muscle, respectively ($^*P < 0.005$ for both Cav-1- and Cav-2-deficient mice). Immediately after birth (P0), Cav-2-deficient mice display a slight, but not significant, increase in SR volume.

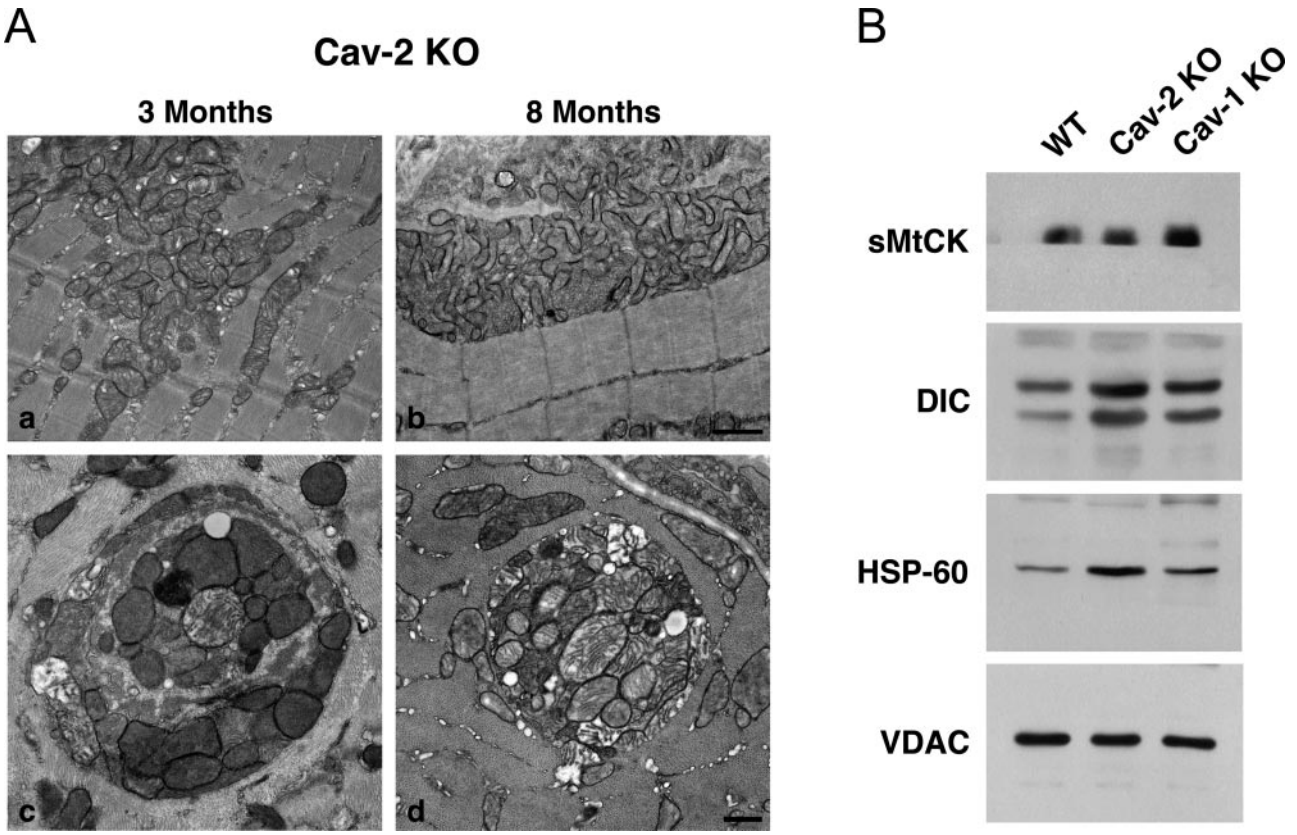

Figure 8. Cav-2-deficient skeletal muscle contains large mitochondrial aggregates. **A:** Electron micrographs of skeletal muscle from 3- and 8-month-old Cav-2-deficient mice. Note the presence of multiple mitochondrial aggregates. Two basic types of mitochondrial aggregates were observed: an amorphous collection (**a** and **b**), which was more prevalent, and a circular organized form (**c** and **d**). Scale bars in **b** and **d** = 500 nm and applies to all four panels. **B:** Immunoblot analysis with mitochondrial markers reveals an increase in DIC and HSP-60 protein levels but not sMtCK or VDAC in Cav-2-deficient skeletal muscle samples compared with WT controls.

see *http://ajp.amjpathol.org*). Interestingly, staining with the three mitochondrial enzymes COX, NADH, and SDH yielded similar results. Although WT muscle sections presented few areas of intense staining, denoting mitochondrial aggregates in a limited numbers of muscle fibers, almost all Cav-2-deficient muscle fibers had very large and dense areas of staining, suggesting the presence of large mitochondrial aggregates in all of the myofibers. Consistent with the histochemical analysis, trichrome staining demonstrated an obvious increase in TA and mitochondrial aggregates in Cav-2-deficient mice (Supplemental Figure 1, see *http://ajp.amjpathol.org*). Interestingly, all muscle fibers with TAs also contained mitochondrial aggregates, whereas other fibers, which did not contain any TAs, still exhibited mitochondrial aggregates. These results suggest a possible correlation between the onset of these two different phenomenons, tubular and mitochondrial aggregates, since they both represent abnormal growth of organelles within the cell.

To determine whether the mitochondria in Cav-2-deficient skeletal muscle were capable of functioning in a normal fashion, the enzymatic activity of various mitochondrial enzymes was examined. Figure 9B represents the mitochondrial activity normalized to citrate synthase activity levels. Interestingly, mitochondrial enzymatic activity levels were normal in Cav-2-deficient muscle, suggesting that Cav-2-deficient mitochondria have the ability to function within normal parameters.

Cav-2-Deficient Skeletal Muscle Displays an Increased Number of Satellite Cells

We show here that Cav-2 deficiency profoundly perturbs the morphology of skeletal muscle, by inducing the formation of tubular aggregates and mitochondrial proliferation/aggregation. However, because Cav-2 is not normally expressed in mature skeletal muscle, such muscular phenotypes were very surprising and raised questions regarding the underlying molecular mechanisms. As such, we decided to evaluate the status of skeletal muscle precursor cells, or satellite cells, which, given their undifferentiated status, still express the non-muscle caveolins Cav-1 and Cav-2. For this purpose, we subjected WT and Cav-2-null skeletal muscle sections to immunofluorescence analysis with an antibody against a satellite cell marker M-cadherin. Figure 10A reveals that Cav-2-deficient myofibers exhibit a significant increase in M-cadherin staining compared with their WT counterparts.

Western blot analysis on skeletal muscle lysates independently showed that M-cadherin expression levels were elevated in Cav-1- and Cav-2-deficient mice

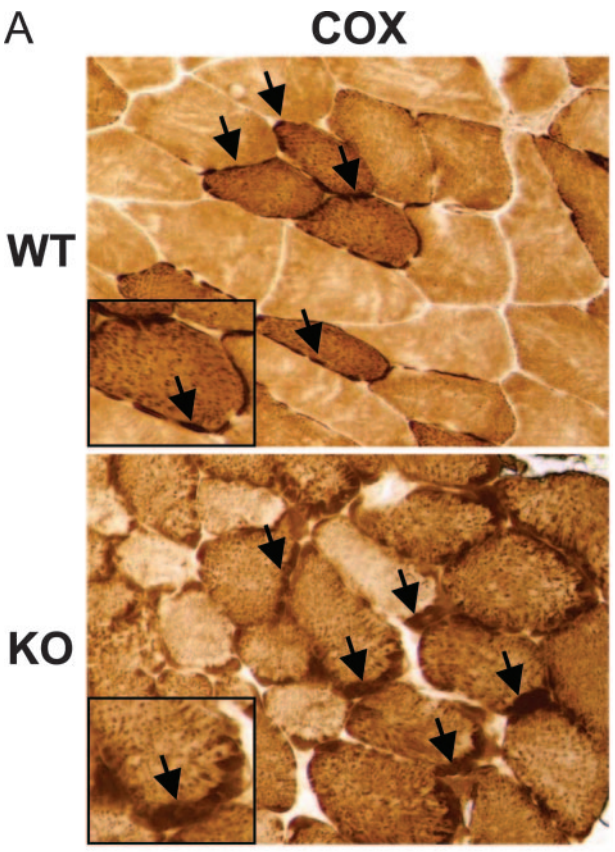

B

Enzyme activity	WT	KO
Cytochrome c oxidase	0.117 +\-0.011	0.138 +\-0.030
Succ. cytochrome c reductase (II+III)	0.014 +\-0.016	0.025 +\-0.017
NADH cytochrome c reductase (I+III)	0.111 +\-0.020	0.124 +\-0.045
NADH deydrogenase (NADH) (I)	0.689 +\-0.086	1.045 +\-0.190
Succinate dehydrogenase (SDH)	0.041 +\-0.004	0.041 +\-0.007

Figure 9. Characterization of mitochondrial function in Cav-2-deficient skeletal muscle. **A:** Cytochrome *c* oxidase (IV) (COX) staining of WT and Cav-2-deficient skeletal muscle. Note the large clusters of mitochondria at the periphery of Cav-2-null muscle fibers (**arrows**). These large aggregates can be seen in some WT fibers; however, the overall number of WT fibers containing the aggregates is lower, and the size of the aggregates is smaller than in Cav-2 KO myofibers. **B:** To determine whether the mitochondria from Cav-2-deficient skeletal muscle functioned normally, the activity of various mitochondrial-specific-enzymes was examined. Although some enzymatic activity levels were somewhat higher in Cav-2-deficient samples, they were not very significantly different, suggesting these mitochondria are capable of functioning normally.

(Figure 10A). We reasoned that increased M-cadherin expression levels could result from abnormal proliferation of M-cadherin expressing cells—satellite cells—in Cav-2-deficient skeletal muscle. Because Cav-2 has been considered an "accessory" protein for Cav-1, this idea is quite novel. There is a single report linking Cav-2 loss of function to increased proliferation: Cav-2-deficient mice were shown to display lung abnormalities, with thickened alveolar septa, with the hyperproliferation of endothelial cells.[20] Nevertheless, the role of Cav-2 in the regulation of cell proliferation and growth remains undefined.

To assess directly whether loss of Cav-2 induces the abnormal proliferation of satellite cells, we performed a double labeling experiment with antibodies against M-cadherin and Cav-1, another marker of satellite cells, on skeletal muscle sections from WT and Cav-2 KO mice. Then, we monitored the number of satellite cells by counting the numbers of M-cadherin- or Cav-1-positive cells. Figure 10B shows a clear increase in the number of M-cadherin- and Cav-1-positive cells in Cav-2-deficient muscle. In addition, note the close co-localization of Cav-1 and M-cadherin within the skeletal muscle. We then proceeded to quantify the number of satellite cells in WT and Cav-2 KO skeletal muscle sections. Interestingly, Figure 10C shows that Cav-2-deficient skeletal muscle displays an increase of 37 and 40% in Cav-1-positive cells and in M-cadherin-positive cells, respectively. These results clearly suggest that loss of Cav-2 disrupts anti-proliferative signals within satellite cells and induces their abnormal proliferation.

Such significant increases in the number of satellite cells could lead to gross abnormalities of the skeletal muscle itself, for example an increase in muscle fiber size. To test this idea, we measured the cross-sectional area of over 600 WT and Cav-2-deficient muscle fibers. Figure 10D reveals that the cross-sectional area of the Cav-2-deficient muscle fibers was significantly enlarged compared with WT fibers (311 versus 249 μm^2).

Cav-2-Deficient Skeletal Muscle Displays a Delay in the Regeneration Process

As Cav-2-deficient skeletal muscle shows satellite cell abnormalities (increased cell number and increased M-cadherin expression), we next examined the capacity of Cav-2-deficient satellite cells to undergo differentiation *in vivo* by studying their regenerative response to a myotoxic substance. The gastrocnemius muscles from age-matched 8-month-old WT and Cav-2-null male mice were injected with a neurotoxic drug, notexin, and harvested either 3 or 7 days after injury. To evaluate their regeneration status, we monitored M-cadherin expression. Figure 11 (top panels) shows that, 3 days after injury, many M-cadherin-positive cells were present both in WT and in Cav-2-deficient skeletal muscle, suggesting that satellite cells are similarly proliferating and that the regenerative process has started in a similar fashion, both in WT and in Cav-2-deficient mice. However, 7 days after injury, the regenerative process was far advanced in WT skeletal muscle compared with their Cav-2-deficient counterparts. Figure 11 (bottom panels) shows the presence of multiple individual M-cadherin-positive fibers in WT sections, suggesting that WT satellite cells have the ability to fuse and generate mature muscle fibers. On the contrary, Cav-2-deficient skeletal muscle still displayed features of damage, with M-cadherin staining being less well defined and few, if any, individual muscle fibers detected. Taken together, these results suggest that Cav-2 ablation

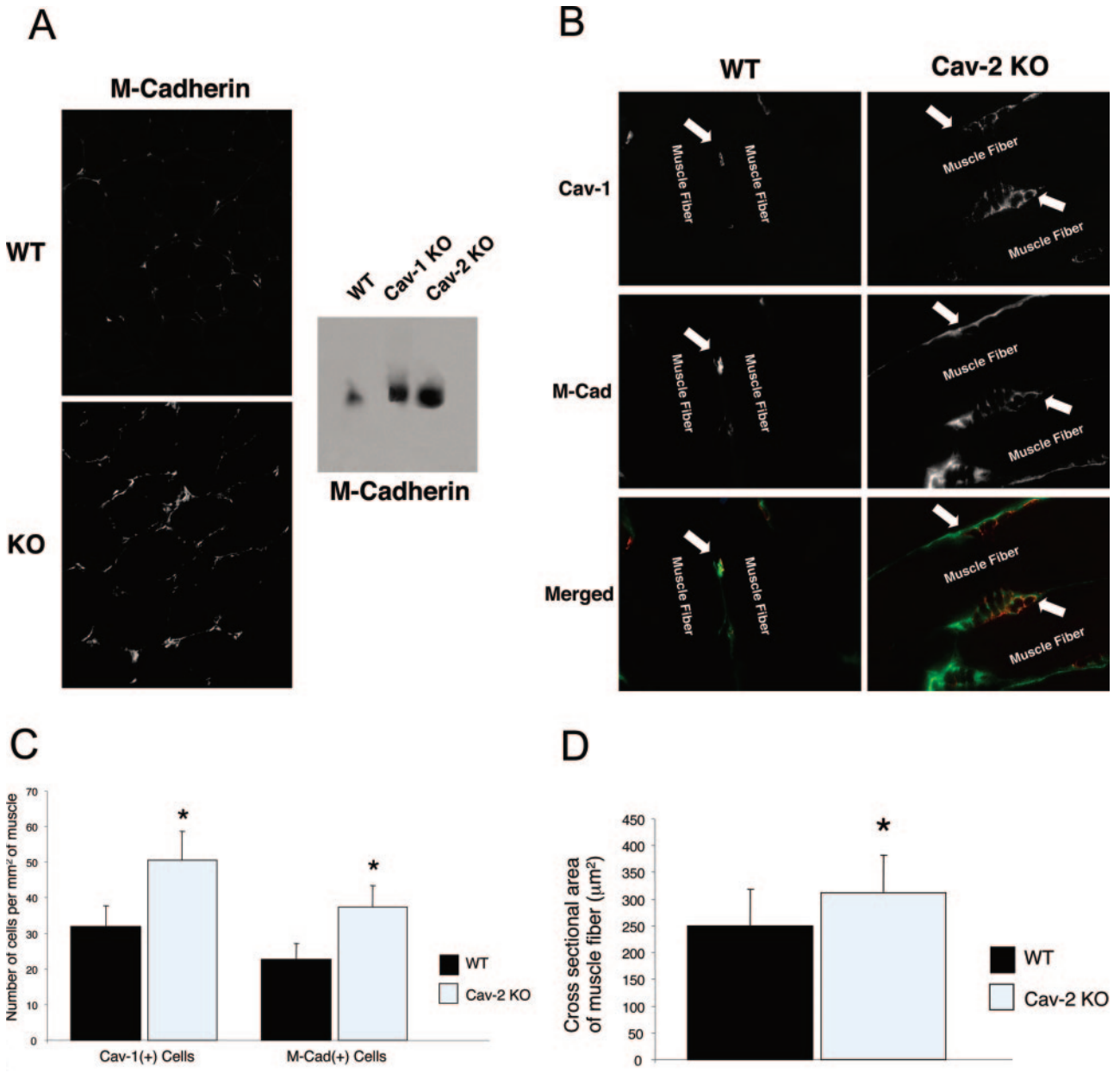

Figure 10. Cav-2-deficient mice display increased numbers of satellite cells and increased muscle fiber size. **A:** Cav-2-deficient mice have increased M-cadherin immuno-reactivity in skeletal muscle sections compared with WT controls. In addition, immunoblot analysis confirms an increase in M-cadherin expression levels in both Cav-1- and Cav-2-deficient mice compared with WT controls. **B:** To confirm that the increase in M-cadherin expression was due to an increase in satellite cell number, skeletal muscle sections were double-labeled with M-cadherin and with a second satellite cell marker, Cav-1. Merged images reveal a co-localization pattern of M-cadherin and Cav-1 and show an increase in the number of satellite cells in Cav-2-deficient skeletal muscles. **C:** Cav-2-deficient skeletal muscles contain an increased number of both Cav-1-positive and M-cadherin-positive cells compared with WT control muscle. Cav-2-deficient muscle had a ~37 and ~40% increase in Cav-1-positive and M-cadherin-positive cells, respectively, when compared with WT muscle ($^*P < 0.05$). **D:** Cav-2-deficient muscle fibers are significantly larger than WT muscle fibers. On average, Cav-2-deficient muscle fibers are ~20% larger than WT muscle fibers, with an average cross-sectional area of 311 μm^2 compared with 249 μm^2 for WT controls ($^*P < 0.005$).

induces the abnormal proliferation of satellite cells, which have an impaired ability to undergo proper regeneration after injury.

Discussion

Caveolae are plasma membrane invaginations found in numerous cell types, including endothelial cells, adipocytes, fibroblasts, type I pneumocytes, and epithelial cells, as well as in all three muscle cells types; ie, skeletal, cardiac, and smooth muscle.[26–31] Although these 50- to 100-nm structures were originally reported to function as endocytic vesicles for the movement of molecules across endothelial cells,[32] subsequent work has demonstrated their involvement in many cellular functions. Importantly, caveolae are enriched in lipid-modified cytoplasmic signaling molecules, including nitric-oxide synthase, Src family tyrosine kinases, and heterotrimeric G proteins,[33,34] thus acting as focal points for the coordination of signal transduction processes at the plasma membrane.[35]

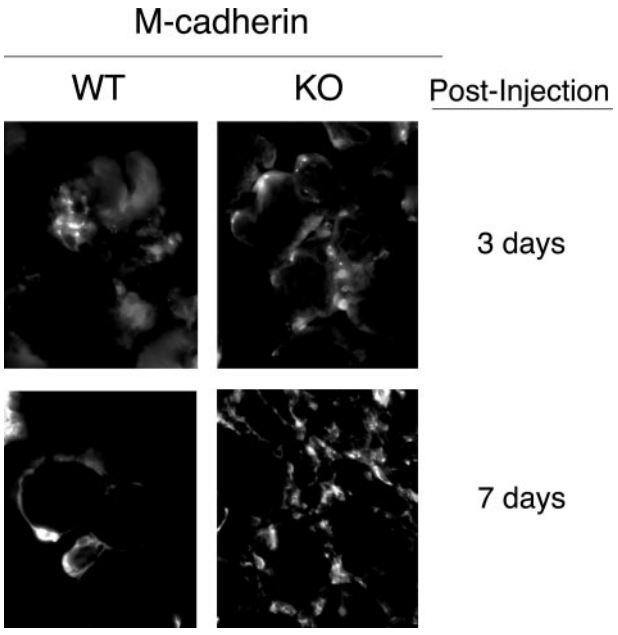

Figure 11. Cav-2-deficient skeletal muscle exhibits an altered response to injury. To evaluate their regenerative capacity, WT and Cav-2-deficient skeletal muscle were locally injected with a neurotoxin, notexin, and harvested at 3 and 7 days after injury. **Top:** Staining with M-cadherin at 3 days after injury. WT and Cav-2-deficient skeletal muscles display an increase in M-cadherin expression, suggesting that both WT and Cav-2-deficient satellite cells have started to proliferate. **Bottom:** Staining with M-cadherin at 7-days after injury. Note the altered response of Cav-2-deficient muscle to damage. Several WT muscle fibers can be identified as individual cells with M-cadherin labeling the plasma membrane, suggesting that WT satellite cells have started to fuse and form mature skeletal muscle fibers. On the contrary, Cav-2-deficient muscle is more disorganized, with large areas of as yet undifferentiated muscle cell precursors. These results suggest that Cav-2-deficient satellite cells display a delay in regenerating skeletal muscle fibers.

The principal structural proteins of caveolae membranes belong to the caveolin gene family, which consists of three members, caveolin-1, -2, and -3.[36–39] Caveolin-1 (Cav-1) and caveolin-3 (Cav-3) share a relatively high degree of identity, whereas caveolin-2 (Cav-2) is the most divergent member of the family. Interestingly, despite the homology between Cav-1 and Cav-3 genes, their expression profiles are vastly different. Endothelial cells, adipocytes, fibroblasts, type I pneumocytes, and epithelial cells highly co-express Cav-1 and -2, whereas Cav-3 is restricted to muscle cell types. Interestingly, smooth muscle cells are the only cell type in which all three proteins are co-expressed, possibly because of its hybrid fibroblast/muscle-like nature. In contrast, Cav-2 expression is directly dependent on Cav-1 expression. Cav-2 requires the presence of Cav-1 for proper membrane targeting and stabilization, such that in the absence of Cav-1, Cav-2 is retained in the endoplasmic reticulum (ER)/Golgi complex and undergoes degradation through a proteaosomal pathway.[19,40] However, Cav-1 expression and function do not rely on Cav-2 expression.

Because Cav-2 has been considered an "accessory" protein that functions in conjunction with Cav-1, the physiological role of Cav-2 remains elusive. The Cav-2 protein sequence contains few of the conserved regions that are believed to be involved in the known functions of Cav-1; ie, membrane attachment,[41] formation of caveolae,[42] and compartmentalization and inhibition of signaling molecules.[43] Currently, the only known physiological roles of Cav-2 are hetero-oligomerization with Cav-1[44] and pulmonary dysfunction observed on Cav-2 deletion in mice.[20]

Phenotypic Characterization of Cav-2 Knockout Skeletal Muscle

In the present study, we describe new unexpected phenotypes in the skeletal muscle of Cav-2-deficient mice. The presence of mitochondrial aggregates and of tubular aggregates in skeletal muscle fibers of male Cav-2 mice at a young age (as early as 3 months) is surprising given that Cav-2 is not expressed in adult skeletal muscle. However, both Cav-1 and Cav-2 are expressed in myoblasts, before terminal differentiation, and in myotube precursor cells, or satellite cells.

The formation of tubular aggregates is not dependent on Cav-3 expression or the formation of caveolae in skeletal muscle, since both seem normal in the Cav-2-deficient mice. In addition, our work clearly demonstrates that tubular aggregates originate mainly from the sarcoplasmic reticulum. This is supported by the fact that TAs in Cav-2-deficient mice contain known SR resident proteins, such as SERCA-1, SERCA-2, GRP-78, and calsequestrin. Interestingly, we also show that loss of Cav-2 induces the mis-localization of calsequestrin from the SR to the plasma membrane.

Early during myofiber development, peripheral coupling between the SR and the plasma membrane occurs. For example, the DHPRα is transiently expressed on the plasma membrane as well as on SR membranes.[45,46] Because Cav-2 is expressed at the plasma membrane in myogenic precursor cells, it is possible that loss of Cav-2 affects the development or maturation of muscle fibers, resulting in the altered localization and expression of SR resident proteins. On the other hand, Cav-2 may be required for the proper localization of certain proteins, such as calsequestrin, and in the absence of Cav-2, calsequestrin is mislocalized to the plasma membrane. For example, in muscular dysgenesis mice, the α1 subunit of the DHP receptor is lacking, resulting in mistargeting of the α2 subunit to the plasma membrane instead of the triad junction.[47] Further work is needed to address directly the relationship between Cav-2 expression and calsequestrin localization.

In all previous studies, including the current study, the appearance of TAs occurs in an age-dependent manner. Although Agbulut et al have shown that many inbred mouse strains examined develop TAs, they do not become abundant until ~10 months of age.[18] The senescence-accelerated SAMP8 mouse and the MRL$^{+/+}$ mouse develop TAs as early as 6 months.[15, 17] However, we show here that Cav-2-deficient mice develop TAs as early as 3 months of age in conjunction with severely dilated SR tubules. As such, Cav-2 KO mice constitute the first well-defined genetic model to study the pathogenesis of tubular aggregate formation.

Tubular Aggregates and Calcium Homeostasis

Several lines of evidence suggest that a defect in Ca^{2+} homeostasis is responsible for the formation of TAs: 1) the SR functions in intracellular Ca^{2+} homeostasis; 2) TAs have been shown to have calcium-loading capabilities;[13] 3) several human skeletal muscle conditions, known to exhibit TA formation, including periodic paralysis and myalgia/cramps syndrome, display perturbed intrasarcoplasmic Ca^{2+} homeostasis;[48, 49] and 4) treatment with Dantrolene, a muscle-specific relaxant that diminishes Ca^{2+} release from the SR, has been shown to provide beneficial effects in patients with a variety of neuromuscular disorders known to contain TAs.[50] Additional indications for a correlation between TA formation and Ca^{2+} homeostasis come from the observations that there is a pronounced difference in Ca^{2+} uptake between type I and type II muscle fibers, that type II fibers have a higher volume percentage of SR (see review[51]), and that TA formation is only seen in type II fibers. In addition, we show that TA formation correlates with enlargement of the SR in Cav-2-deficient mice. Taken together, these findings support the idea that TAs may represent an adaptive mechanism to compensate for increased intracellular levels of calcium and to avoid muscle fibers hypercontraction and necrosis. In response to the increase in intracellular levels of Ca^{2+}, the terminal cisternae of the SR would undergo hypertrophy with a subsequent rearrangement into TAs in an attempt to act as a calcium sink and prevent irreversible contraction of the fiber or cell death.

How does a Cav-2 deficiency relate to calcium signaling and regulation? Several lines of evidence suggest that caveolae constitute a major site of Ca^{2+} entry. For example, endothelial Ca^{2+} waves preferentially originate at specific caveolin-rich edges, and molecules that regulate Ca^{2+} influx into cells, such as the inositol 1,4,5-trisphosphate receptor-like protein, and the plasmalemmal Ca^{2+}-ATPase localize to caveolae.[52–54] Although loss of Cav-2 does not affect caveolae formation per se, it may still affect caveolae function in regulating Ca^{2+} influx into cells. As such, Cav-2-deficient caveolae may provoke alterations in Ca^{2+} signaling and induce an abnormal accumulation of Ca^{2+} in the cytosol. In this view, TAs would develop to compensate for the increased intracellular Ca^{2+} levels. The idea that Cav-2 modulates the dynamics of Cav-1-dependent caveolae is not completely new. For example, Cav-2 phosphorylation on serine 23 and 36 was shown to be necessary for plasma membrane attachment of Cav-1-positive caveolae in prostate cancer cells, suggesting that although not necessary per se for caveolae formation, Cav-2 expression is still needed for specialized caveolar functions.[55]

Tubular Aggregates and Mitochondrial Dysfunction

Several groups have shown a correlation between mitochondrial dysfunction and the TA formation.[14,56] We also show a link between TA formation and mitochondrial abnormalities. As early as 3 months of age, Cav-2-deficient mice develop large mitochondrial aggregates and atypical mitochondrial clusters not seen in age-matched WT controls. Interestingly, TA formation and SR dilatation coincide with the appearance of mitochondrial aggregates, suggesting interdependence between these conditions. Immunoblot analysis of Cav-2-deficient skeletal muscle shows increased levels of DIC and HSP-60 proteins, whereas the levels of other mitochondria-specific markers are unchanged. Mitochondria are extremely sensitive to increased intracellular calcium levels. For example, in Duchenne's muscular dystrophy and *mdx* mice, the loss of dystrophin destabilizes the plasma membrane, leading to an increase in intracellular levels of Ca^{2+}[57] and subsequent disruption of proper mitochondrial function.[58,59]

How mitochondrial function and tubular aggregate formation are connected remains unclear. However, the appearance of TAs and mitochondrial aggregates in Cav-2-deficient mice earlier than in any other mouse strain should allow for a detailed examination and identification of the underlying molecular mechanisms. The fact that at 8 months of age all muscle fibers with TA also contain mitochondrial aggregates, whereas other fibers that do not contain any TA still exhibit mitochondrial aggregates, suggests the establishment of a temporal progression between these two phenotypes. As such, we propose that the formation of mitochondrial aggregates may precede the formation of tubular aggregates.

Tubular Aggregates and Skeletal Muscle Regeneration

Skeletal muscle regeneration is a complex, multistep process in which satellite cells are activated, by signals from necrotic muscle cells, to become myoblasts. These myoblasts then replicate and fuse to form myotubes, which then differentiate to become fully formed muscle fibers (see review[60]). We show here that Cav-2 is normally expressed in myogenic precursor muscle cells and that loss of Cav-2 induces abnormally high numbers of satellite cells in skeletal muscle. Our findings are surprising because little is known about the role of Cav-2 in the regulation of cell proliferation. A previous report has shown that Cav-2-null mice display lung abnormalities, with hyperproliferation of lung endothelial cells. That and our current study are the first to suggest that Cav-2 may play a critical role in controlling cell proliferation. Constant satellite cell hyperproliferation and subsequent incomplete differentiation-regeneration cycles may underlie the pathogenesis of tubular and mitochondrial aggregate formation. This hypothesis is corroborated by the fact that tubular and mitochondrial aggregates are absent in newborn mice—in which the defects in differentiation-regeneration cycles have not yet damaged the muscle—and that their numbers increase with aging. In addition, we show here that Cav-2-deficient skeletal muscle displays an obvious delay in regeneration after injury. Interestingly, 3 days after injury, Cav-2-deficient satellite cells have the ability to undergo proliferation but exhibit an inability to form differentiated myofibers. It is very likely

that Cav-2-deficient myogenic precursor cells are fully committed into a proliferative pathway and are unable to undergo differentiation, thus impairing their ability to respond to muscle injury and repair skeletal muscle fibers in a proper fashion.

In conclusion, we have identified several novel defects in the skeletal muscle of Cav-2-deficient mice, which seem to be independent of Cav-1 expression levels. These findings open new avenues for further understanding of the physiological functions of Cav-2 in controlling cell proliferation and differentiation in skeletal muscle. In addition, Cav-2-deficient mice will provide an interesting new source for the potential biochemical purification of tubular aggregates.

References

1. Engel WK: Mitochondrial aggregates in muscle disease. J Histochem Cytochem 1964, 12:46–48
2. Gruner JE: Anomalies of the sarcoplasmic reticulum and proliferation of tubules in the muscle in familial periodic paralysis. C R Seances Soc Biol Fil (French) 1966, 160:193–195
3. Engel WK, Bishop DW, Cunningham GG: Tubular aggregates in type II muscle fibers: ultrastructural and histochemical correlation. J Ultrastruct Res 1970, 31:507–525
4. de Groot JG, Arts WF: Familial myopathy with tubular aggregates. J Neurol 1982, 227:35–41
5. Rohkamm R, Boxler K, Ricker K, Jerusalem F: A dominantly inherited myopathy with excessive tubular aggregates. Neurology 1983, 33:331–336
6. Martin JJ, Ceuterick C, Van Goethem G: On a dominantly inherited myopathy with tubular aggregates. Neuromuscul Disord 1997, 7:512–520
7. Alonso-Losada G, Cimas I, Pego R, La Torre P, Teijeira S, Navarro C: Isolated progressive muscle weakness with tubular aggregates. Clin Neuropathol 1998, 17:50–54
8. Dobkin BH, Verity MA: Familial neuromuscular disease with type 1 fiber hypoplasia, tubular aggregates, cardiomyopathy, and myasthenic features. Neurology 1978, 28:1135–1140
9. Morgan-Hughes JA, Lecky BR, Landon DN, Murray NM: Alterations in the number and affinity of junctional acetylcholine receptors in a myopathy with tubular aggregates. A newly recognized receptor defect. Brain 1981, 104:279–295
10. Brumback RA, Staton RD, Susag ME: Exercise-induced pain, stiffness, and tubular aggregation in skeletal muscle. J Neurol Neurosurg Psychiatry 1981, 44:250–254
11. Takizawa S, Ishihara T, Shinohara Y: [A case of hypokalemic periodic paralysis with tubular aggregates in type 2A fibers and type 2B fibers]. Rinsho Shinkeigaku 1986, 26:81–86
12. Sipilä I, Simell O, Rapola J, Sainio K, Tuuteri L: Gyrate atrophy of the choroid and retina with hyperornithinemia: tubular aggregates and type 2 fiber atrophy in muscle. Neurology 1979, 29:996–1005
13. Salviati G, Pierobon-Bormioli S, Betto R, Damiani E, Angelini C, Ringel SP, Salvatori S, Margreth A: Tubular aggregates: sarcoplasmic reticulum origin, calcium storage ability, and functional implications. Muscle Nerve 1985, 8:299–306
14. Novotová M, Zahradnik I, Brochier G, Pavlovicova M, Bigard X, Ventura-Clapier R: Joint participation of mitochondria and sarcoplasmic reticulum in the formation of tubular aggregates in gastrocnemius muscle of CK−/− mice. Eur J Cell Biol 2002, 81:101–106
15. Nishikawa T, Takahashi JA, Matsushita T, Ohnishi K, Higuchi K, Hashimoto N, Hosokawa M: Tubular aggregates in the skeletal muscle of the senescence-accelerated mouse; SAM. Mech Ageing Dev 2000, 114:89–99
16. Craig ID, Allen IV: Tubular aggregates in murine dystrophy heterozygotes. Muscle Nerve 1980, 3:134–140
17. Kuncl RW, Pestronk A, Lane J, Alexander E: The MRL +/+ mouse: a new model of tubular aggregates which are gender- and age-related. Acta Neuropathol (Berl) 1989, 78:615–620
18. Agbulut O, Destombes J, Thiesson D, Butler-Browne G: Age-related appearance of tubular aggregates in the skeletal muscle of almost all male inbred mice. Histochem Cell Biol 2000, 114:477–481
19. Razani B, Engelman JA, Wang XB, Schubert W, Zhang XL, Marks CB, Macaluso F, Russell RG, Li M, Pestell RG, Di Vizio D, Hou Jr H, Kneitz B, Lagaud G, Christ GJ, Edelmann W, Lisanti MP: Caveolin-1 null mice are viable but show evidence of hyperproliferative and vascular abnormalities. J Biol Chem 2001, 276:38121–38138
20. Razani B, Wang XB, Engelman JA, Battista M, Lagaud G, Zhang XL, Kneitz B, Hou Jr H, Christ GJ, Edelmann W, Lisanti MP: Caveolin-2-deficient mice show evidence of severe pulmonary dysfunction without disruption of caveolae. Mol Cell Biol 2002, 22:2329–2344
21. Galbiati F, Engelman JA, Volonte D, Zhang XL, Minetti C, Li M, Hou H, Jr., Kneitz B, Edelmann W, Lisanti MP: Caveolin-3 null mice show a loss of caveolae, changes in the microdomain distribution of the dystrophin-glycoprotein complex, and T-tubule abnormalities. J Biol Chem 2001, 276:21425–21433
22. Park DS, Lee H, Frank PG, Razani B, Nguyen AV, Parlow AF, Russell RG, Hulit J, Pestell RG, Lisanti MP: Caveolin-1-deficient mice show accelerated mammary gland development during pregnancy, premature lactation, and hyperactivation of the Jak-2/STAT5a signaling cascade. Mol Biol Cell 2002, 13:3416–3430
23. Tritschler HJ, Bonilla E, Lombes A, Andreetta F, Servidei S, Schneyder B, Miranda AF, Schon EA, Kadenbach B, DiMauro S: Differential diagnosis of fatal and benign cytochrome c oxidase-deficient myopathies of infancy: an immunohistochemical approach. Neurology 1991, 41:300–305
24. DiMauro S, Servidei S, Zeviani M, DiRocco M, DeVivo DC, DiDonato S, Uziel G, Berry K, Hoganson G, Johnsen SD: Cytochrome c oxidase deficiency in Leigh syndrome. Ann Neurol 1987, 22:498–506
25. Serrano M, Lee H, Chin L, Cordon-Cardo C, Beach D, DePinho RA: Role of the INK4a locus in tumor suppression and cell mortality. Cell 1996, 85:27–37
26. Palade GE: Fine structure of blood capillaries. J Appl Physiol 1953, 24:1424
27. Napolitano LM: The differentiation of white adipose cells. An electron microscope study. J Cell Biol 1963, 18:663–679
28. Mobley BA, Eisenberg BR: Sizes of components in frog skeletal muscle measured by methods of stereology. J Gen Physiol 1975, 66:31–45
29. Gabella G: Quantitative morphological study of smooth muscle cells of the guinea-pig taenia coli. Cell Tissue Res 1976, 170:161–186
30. Gil J: Number and distribution of plasmalemmal vesicles in the lung. Fed Proc 1983, 42:2414–2418
31. Song KS, Scherer PE, Tang Z, Okamoto T, Li S, Chafel M, Chu C, Kohtz DS, Lisanti MP: Expression of caveolin-3 in skeletal, cardiac, and smooth muscle cells. Caveolin-3 is a component of the sarcolemma and co-fractionates with dystrophin and dystrophin-associated glycoproteins. J Biol Chem 1996, 271:15160–15165
32. Simionescu N: Cellular aspects of transcapillary exchange. Physiol Rev 1983, 63:1536–1560
33. Couet J, Li S, Okamoto T, Scherer PE, Lisanti MP: Molecular and cellular biology of caveolae: paradoxes and plasticities. Trends Cardiovasc Med 1997, 7:103–110
34. Lisanti MP, Scherer P, Tang Z-L, Sargiacomo M: Caveolae, caveolin and caveolin-rich membrane domains: a signalling hypothesis. Trends Cell Biol 1994, 4:231–235
35. Smart EJ, Graf GA, McNiven MA, Sessa WC, Engelman JA, Scherer PE, Okamoto T, Lisanti MP: Caveolins, liquid-ordered domains, and signal transduction. Mol Cell Biol 1999, 19:7289–7304
36. Glenney JR, Jr., Zokas L: Novel tyrosine kinase substrates from Rous sarcoma virus-transformed cells are present in the membrane skeleton. J Cell Biol 1989, 108:2401–2408
37. Rothberg KG, Heuser JE, Donzell WC, Ying Y, Glenney JR, Anderson RGW: Caveolin, a protein component of caveolae membrane coats. Cell 1992, 68:673–682
38. Scherer PE, Okamoto T, Chun M, Nishimoto I, Lodish HF, Lisanti MP: Identification, sequence and expression of caveolin-2 defines a caveolin gene family. Proc. Natl Acad Sci USA 1996, 93: 131–135
39. Tang Z-L, Scherer PE, Okamoto T, Song K, Chu C, Kohtz DS, Nishimoto I, Lodish HF, Lisanti MP: Molecular cloning of caveolin-3, a novel member of the caveolin gene family expressed predominantly in muscle. J Biol Chem 1996, 271:2255–2261

40. Parolini I, Sargiacomo M, Galbiati F, Rizzo G, Grignani F, Engelman JA, Okamoto T, Ikezu T, Scherer PE, Mora R, Rodriguez-Boulan E, Peschle C, Lisanti MP: Expression of caveolin-1 is required for the transport of caveolin-2 to the plasma membrane. Retention of caveolin-2 at the level of the Golgi complex. J Biol Chem 1999, 274:25718–25725
41. Schlegel A, Lisanti MP: A molecular dissection of caveolin-1 membrane attachment and oligomerization. Two separate regions of the caveolin-1 C-terminal domain mediate membrane binding and oligomer/oligomer interactions in vivo. J Biol Chem 2000, 275:21605–21617
42. Sargiacomo M, Scherer PE, Tang Z-L, Kubler E, Song KS, Sanders MC, Lisanti MP: Oligomeric structure of caveolin: implications for caveolae membrane organization. Proc Natl Acad Sci USA 1995, 92:9407–9411
43. Razani B, Rubin CS, Lisanti MP: Regulation of cAMP-mediated signal transduction via interaction of caveolins with the catalytic subunit of protein kinase A. J Biol Chem 1999, 274:26353–26360
44. Scherer PE, Lewis RY, Volonte D, Engelman JA, Galbiati F, Couet J, Kohtz DS, van Donselaar E, Peters P, Lisanti MP: Cell-type and tissue-specific expression of caveolin-2. Caveolins 1 and 2 co-localize and form a stable hetero-oligomeric complex in vivo. J Biol Chem 1997, 272:29337–29346
45. Flucher BE: Structural analysis of muscle development: transverse tubules, sarcoplasmic reticulum, and the triad. Dev Biol 1992, 154:245–260
46. Yuan SH, Arnold W, Jorgensen AO: Biogenesis of transverse tubules and triads: immunolocalization of the 1,4-dihydropyridine receptor, TS28, and the ryanodine receptor in rabbit skeletal muscle developing in situ. J Cell Biol 1991, 112:289–301
47. Flucher BE, Phillips JL, Powell JA: Dihydropyridine receptor alpha subunits in normal and dysgenic muscle in vitro: expression of alpha 1 is required for proper targeting and distribution of alpha 2. J Cell Biol 1991, 115:1345–1356
48. Taylor DJ, Brosnan MJ, Arnold DL, Bore PJ, Styles P, Walton J, Radda GK: Ca2+-ATPase deficiency in a patient with an exertional muscle pain syndrome. J Neurol Neurosurg Psychiatry 1988, 51:1425–1433
49. Tirasophon W, Welihinda AA, Kaufman RJ: A stress response pathway from the endoplasmic reticulum to the nucleus requires a novel bifunctional protein kinase/endoribonuclease (Ire1p) in mammalian cells. Genes Dev 1998, 12:1812–1824
50. Vissing J, Schmalbrunch H, Haller RG, Clausen T: Muscle phosphoglycerate mutase deficiency with tubular aggregates: effect of dantrolene. Ann Neurol 1999, 46:274–277
51. Pette D, Staron RS: Cellular and molecular diversities of mammalian skeletal muscle fibers. Rev Physiol Biochem Pharmacol 1990, 116:1–76
52. Isshiki M, Ando J, Korenaga R, Kogo H, Fujimoto T, Fujita T, Kamiya A: Endothelial Ca2+ waves preferentially originate at specific loci in caveolin-rich cell edges. Proc Natl Acad Sci USA 1998, 95:5009–5014
53. Fujimoto T, Nakade S, Miyawaki A, Mikoshiba K, Ogawa K: Localization of inositol 1,4,5-trisphosphate receptor-like protein in plasmalemmal caveolae. J Cell Biol 1992, 119:1507–1513
54. Fujimoto T: Calcium pump of the plasma membrane is localized in caveolae. J Cell Biol 1993, 120:1147–1157
55. Sowa G, Pypaert M, Fulton D, Sessa WC: The phosphorylation of caveolin-2 on serines 23 and 36 modulates caveolin-1-dependent caveolae formation. Proc Natl Acad Sci USA 2003, 100: 6511–6516
56. Steeghs K, Benders A, Oerlemans F, de Haan A, Heerschap A, Ruitenbeek W, Jost C, van Deursen J, Perryman B, Pette D, Bruckwilder M, Koudijs J, Jap P, Veerkamp J, Wieringa B: Altered Ca2+ responses in muscles with combined mitochondrial and cytosolic creatine kinase deficiencies. Cell 1997, 89:93–103
57. Duncan CJ: Dystrophin and the integrity of the sarcolemma in Duchenne muscular dystrophy. Experientia 1989, 45:175–177
58. Even PC, Decrouy A, Chinet A: Defective regulation of energy metabolism in mdx-mouse skeletal muscles. J Biochem 1994, 304:649–654
59. Kuznetsov AV, Winkler K, Wiedemann FR, von Bossanyi P, Dietzmann K, Kunz WS: Impaired mitochondrial oxidative phosphorylation in skeletal muscle of the dystrophin-deficient mdx mouse. Mol Cell Biochem 1998, 183:87–96
60. Grounds M: Towards understanding skeletal muscle regeneration. Path Res Pract 1991, 187:1–22